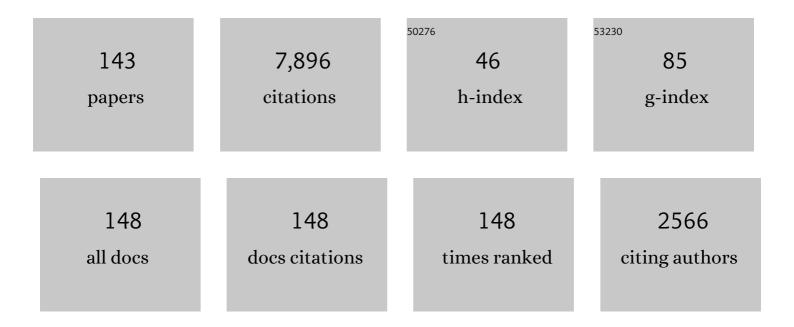
Michael G Henderson

List of Publications by Year in descending order

Source: https://exaly.com/author-pdf/9563343/publications.pdf Version: 2024-02-01



#	Article	IF	CITATIONS
1	Rapid local acceleration of relativistic radiation-belt electrons by magnetospheric chorus. Nature, 2013, 504, 411-414.	27.8	608
2	The Magnetic Electron Ion Spectrometer (MagEIS) Instruments Aboard the Radiation Belt Storm Probes (RBSP) Spacecraft. Space Science Reviews, 2013, 179, 383-421.	8.1	491
3	Electron Acceleration in the Heart of the Van Allen Radiation Belts. Science, 2013, 341, 991-994.	12.6	463
4	Science Goals and Overview of the Radiation Belt Storm Probes (RBSP) Energetic Particle, Composition, and Thermal Plasma (ECT) Suite on NASA's Van Allen Probes Mission. Space Science Reviews, 2013, 179, 311-336.	8.1	463
5	Helium, Oxygen, Proton, and Electron (HOPE) Mass Spectrometer for the Radiation Belt Storm Probes Mission. Space Science Reviews, 2013, 179, 423-484.	8.1	459
6	A Long-Lived Relativistic Electron Storage Ring Embedded in Earth's Outer Van Allen Belt. Science, 2013, 340, 186-190.	12.6	216
7	Geomagnetic storms driven by ICME- and CIR-dominated solar wind. Journal of Geophysical Research, 2006, 111, .	3.3	199
8	Are north-south aligned auroral structures an ionospheric manifestation of bursty bulk flows?. Geophysical Research Letters, 1998, 25, 3737-3740.	4.0	186
9	Evolution and slow decay of an unusual narrow ring of relativistic electrons near L ~ 3.2 following the September 2012 magnetic storm. Geophysical Research Letters, 2013, 40, 3507-3511.	4.0	150
10	On the relationship between relativistic electron flux and solar wind velocity: Paulikas and Blake revisited. Journal of Geophysical Research, 2011, 116, n/a-n/a.	3.3	148
11	Coronal mass ejections, magnetic clouds, and relativistic magnetospheric electron events: ISTP. Journal of Geophysical Research, 1998, 103, 17279-17291.	3.3	144
12	Van Allen Probes observation of localized drift resonance between poloidal mode ultraâ€low frequency waves and 60 keV electrons. Geophysical Research Letters, 2013, 40, 4491-4497.	4.0	127
13	Gradual diffusion and punctuated phase space density enhancements of highly relativistic electrons: Van Allen Probes observations. Geophysical Research Letters, 2014, 41, 1351-1358.	4.0	127
14	Cassini plasma spectrometer thermal ion measurements in Saturn's inner magnetosphere. Journal of Geophysical Research, 2008, 113, .	3.3	120
15	Modeling radiation belt electron dynamics during GEM challenge intervals with the DREAM3D diffusion model. Journal of Geophysical Research: Space Physics, 2013, 118, 6197-6211.	2.4	111
16	On the cause and extent of outer radiation belt losses during the 30 September 2012 dropout event. Journal of Geophysical Research: Space Physics, 2014, 119, 1530-1540.	2.4	110
17	The relativistic electron response at geosynchronous orbit during the January 1997 magnetic storm. Journal of Geophysical Research, 1998, 103, 17559-17570.	3.3	104
18	Competing source and loss mechanisms due to waveâ€particle interactions in Earth's outer radiation belt during the 30 September to 3 October 2012 geomagnetic storm. Journal of Geophysical Research: Space Physics, 2014, 119, 1960-1979.	2.4	103

#	Article	IF	CITATIONS
19	First energetic neutral atom images from Polar. Geophysical Research Letters, 1997, 24, 1167-1170.	4.0	101
20	Magnetospheric and auroral activity during the 18 April 2002 sawtooth event. Journal of Geophysical Research, 2006, 111, .	3.3	100
21	Highly relativistic radiation belt electron acceleration, transport, and loss: Large solar storm events of March and June 2015. Journal of Geophysical Research: Space Physics, 2016, 121, 6647-6660.	2.4	93
22	Modeling inward diffusion and slow decay of energetic electrons in the Earth's outer radiation belt. Geophysical Research Letters, 2015, 42, 987-995.	4.0	87
23	Plasma in Saturn's nightside magnetosphere and the implications for global circulation. Planetary and Space Science, 2009, 57, 1714-1722.	1.7	85
24	Observational evidence for an inside-out substorm onset scenario. Annales Geophysicae, 2009, 27, 2129-2140.	1.6	81
25	Plasmoids in Saturn's magnetotail. Journal of Geophysical Research, 2008, 113, .	3.3	79
26	A background correction algorithm for Van Allen Probes MagEIS electron flux measurements. Journal of Geophysical Research: Space Physics, 2015, 120, 5703-5727.	2.4	78
27	Dynamic Radiation Environment Assimilation Model: DREAM. Space Weather, 2012, 10, .	3.7	74
28	Observations of magnetospheric substorms occurring with no apparent solar wind/IMF trigger. Journal of Geophysical Research, 1996, 101, 10773-10791.	3.3	72
29	Reproducing the observed energyâ€dependent structure of Earth's electron radiation belts during storm recovery with an eventâ€specific diffusion model. Geophysical Research Letters, 2016, 43, 5616-5625.	4.0	71
30	Substorms during the 10â \in "11 August 2000 sawtooth event. Journal of Geophysical Research, 2006, 111, .	3.3	69
31	Thermal ion flow in Saturn's inner magnetosphere measured by the Cassini plasma spectrometer: A signature of the Enceladus torus?. Geophysical Research Letters, 2009, 36, .	4.0	68
32	The May 2-3, 1986 CDAW-9C interval: A sawtooth event. Geophysical Research Letters, 2004, 31, n/a-n/a.	4.0	63
33	Energetic particle injections to geostationary orbit: Relationship to flow bursts and magnetospheric state. Journal of Geophysical Research, 2012, 117, .	3.3	63
34	The storm-substorm relationship: Ion injections in geosynchronous measurements and composite energetic neutral atom images. Journal of Geophysical Research, 2001, 106, 5833-5844.	3.3	62
35	Statistical properties of the surfaceâ€charging environment at geosynchronous orbit. Space Weather, 2013, 11, 237-244.	3.7	62
36	Global Threeâ€Ðimensional Simulation of Earth's Dayside Reconnection Using a Twoâ€Way Coupled Magnetohydrodynamics With Embedded Particleâ€inâ€Cell Model: Initial Results. Journal of Geophysical Research: Space Physics, 2017, 122, 10,318.	2.4	62

#	Article	IF	CITATIONS
37	First medium energy neutral atom (MENA) Images of Earth's magnetosphere during substorm and storm-time. Geophysical Research Letters, 2001, 28, 1147-1150.	4.0	61
38	Observations of the impenetrable barrier, the plasmapause, and the VLF bubble during the 17 March 2015 storm. Journal of Geophysical Research: Space Physics, 2016, 121, 5537-5548.	2.4	59
39	Plasma sheet access to the inner magnetosphere. Journal of Geophysical Research, 2001, 106, 5845-5858.	3.3	58
40	Global energetic neutral atom (ENA) measurements and their association with theDstindex. Geophysical Research Letters, 1997, 24, 3173-3176.	4.0	53
41	IMAGE, POLAR, and geosynchronous observations of substorm and ring current ion injection. Geophysical Monograph Series, 2003, , 91-101.	0.1	52
42	The trapping of equatorial magnetosonic waves in the Earth's outer plasmasphere. Geophysical Research Letters, 2014, 41, 6307-6313.	4.0	51
43	Characterizing the 18 April 2002 storm-time sawtooth events using ground magnetic data. Journal of Geophysical Research, 2006, 111, .	3.3	50
44	Simulation of energyâ€dependent electron diffusion processes in the Earth's outer radiation belt. Journal of Geophysical Research: Space Physics, 2016, 121, 4217-4231.	2.4	50
45	Fast Diffusion of Ultrarelativistic Electrons in the Outer Radiation Belt: 17 March 2015 Storm Event. Geophysical Research Letters, 2018, 45, 10874-10882.	4.0	49
46	A Statistical Survey of Radiation Belt Dropouts Observed by Van Allen Probes. Geophysical Research Letters, 2018, 45, 8035-8043.	4.0	49
47	The Global Positioning System constellation as a space weather monitor: Comparison of electron measurements with Van Allen Probes data. Space Weather, 2016, 14, 76-92.	3.7	48
48	Investigating the source of nearâ€relativistic and relativistic electrons in Earth's inner radiation belt. Journal of Geophysical Research: Space Physics, 2017, 122, 695-710.	2.4	48
49	Cassini detection of waterâ€group pickâ€up ions in the Enceladus torus. Geophysical Research Letters, 2008, 35, .	4.0	47
50	Comparative statistical analysis of storm time activations and sawtooth events. Journal of Geophysical Research, 2007, 112, n/a-n/a.	3.3	46
51	Energetic Particle Data From the Global Positioning System Constellation. Space Weather, 2017, 15, 283-289.	3.7	46
52	An empirical model of electron and ion fluxes derived from observations at geosynchronous orbit. Space Weather, 2015, 13, 233-249.	3.7	44
53	An improved empirical model of electron and ion fluxes at geosynchronous orbit based on upstream solar wind conditions. Space Weather, 2016, 14, 511-523.	3.7	42
54	Northward field excursions in Saturn's magnetotail and their relationship to magnetospheric periodicities. Geophysical Research Letters, 2009, 36, .	4.0	41

#	Article	IF	CITATIONS
55	Auroral Substorms, Poleward Boundary Activations, Auroral Streamers, Omega Bands, and Onset Precursor Activity. Geophysical Monograph Series, 0, , 39-54.	0.1	41
56	Cluster observations in the inner magnetosphere during the 18 April 2002 sawtooth event: Dipolarization and injection at <i>r</i> = 4.6 <i>R</i> _{<i>E</i>} . Journal of Geophysical Research, 2007, 112, .	3.3	40
57	Analyzing electric field morphology through data-model comparisons of the Geospace Environment Modeling Inner Magnetosphere/Storm Assessment Challenge events. Journal of Geophysical Research, 2006, 111, .	3.3	37
58	REPAD: An empirical model of pitch angle distributions for energetic electrons in the Earth's outer radiation belt. Journal of Geophysical Research: Space Physics, 2014, 119, 1693-1708.	2.4	37
59	Observations and Fokkerâ€Planck Simulations of the <i>L</i> â€Shell, Energy, and Pitch Angle Structure of Earth's Electron Radiation Belts During Quiet Times. Journal of Geophysical Research: Space Physics, 2019, 124, 1125-1142.	2.4	37
60	SpacePy - A Python-based Library of Tools for the Space Sciences. , 2010, , .		36
61	Interpretation of optical substorm onset observations. Journal of Atmospheric and Solar-Terrestrial Physics, 1993, 55, 1159-1170.	0.9	34
62	The auroral distribution and its mapping according to substorm phase. Journal of Atmospheric and Solar-Terrestrial Physics, 1993, 55, 1741-1762.	0.9	34
63	The plasma environment inside geostationary orbit: A Van Allen Probes HOPE survey. Journal of Geophysical Research: Space Physics, 2017, 122, 9207-9227.	2.4	34
64	Van Allen Probes observations of direct waveâ€particle interactions. Geophysical Research Letters, 2014, 41, 1869-1875.	4.0	32
65	Magnetotail behavior during storm time "sawtooth injections― Journal of Geophysical Research, 2004, 109, .	3.3	31
66	Observations of Changes to the Auroral Distribution Prior to Substorm Onset. Geophysical Monograph Series, 0, , 257-275.	0.1	31
67	Tail-dominated storm main phase: 31 March 2001. Journal of Geophysical Research, 2003, 108, .	3.3	29
68	A statistical study of magnetic dipolarization for sawtooth events and isolated substorms at geosynchronous orbit with GOES data. Annales Geophysicae, 2006, 24, 3481-3490.	1.6	29
69	Empirical modeling of 3â€D forceâ€balanced plasma and magnetic field structures during substorm growth phase. Journal of Geophysical Research: Space Physics, 2015, 120, 6496-6513.	2.4	29
70	Startâ€toâ€end global imaging of a sunward propagating, SAPSâ€associated giant undulation event. Journal of Geophysical Research, 2010, 115, .	3.3	27
71	Phase Space Density matching of relativistic electrons using the Van Allen Probes: REPT results. Geophysical Research Letters, 2013, 40, 4798-4802.	4.0	27
72	Calculation of Last Closed Drift Shells for the 2013 GEM Radiation Belt Challenge Events. Journal of Geophysical Research: Space Physics, 2018, 123, 9597-9611.	2.4	27

#	Article	IF	CITATIONS
73	The impact of cold electrons and cold ions in magnetospheric physics. Journal of Atmospheric and Solar-Terrestrial Physics, 2021, 220, 105599.	1.6	27
74	Charge exchange contribution to the decay of the ring current, measured by energetic neutral atoms (ENAs). Journal of Geophysical Research, 2001, 106, 1931-1937.	3.3	26
75	Nearâ€Earth substorm features from multiple satellite observations. Journal of Geophysical Research, 2008, 113, .	3.3	26
76	Modeling gradual diffusion changes in radiation belt electron phase space density for the March 2013 Van Allen Probes case study. Journal of Geophysical Research: Space Physics, 2014, 119, 8396-8403.	2.4	24
77	PreMevE: New Predictive Model for Megaelectronâ€Volt Electrons Inside Earth's Outer Radiation Belt. Space Weather, 2019, 17, 438-454.	3.7	24
78	The latitudinal variation of geoelectromagnetic disturbances during large (<i>Dst</i> â‰ ≇ `100ÂnT) geomagnetic storms. Space Weather, 2016, 14, 668-681.	3.7	23
79	Physical Processes of Meso-Scale, Dynamic Auroral Forms. Space Science Reviews, 2020, 216, 1.	8.1	23
80	Current sheet scattering and ion isotropic boundary under 3â€D empirical forceâ€balanced magnetic field. Journal of Geophysical Research: Space Physics, 2014, 119, 8202-8211.	2.4	22
81	Rice Convection Model simulation of the 18 April 2002 sawtooth event and evidence for interchange instability. Journal of Geophysical Research, 2008, 113, .	3.3	21
82	The March 2015 Superstorm Revisited: Phase Space Density Profiles and Fast ULF Wave Diffusive Transport. Journal of Geophysical Research: Space Physics, 2019, 124, 1143-1156.	2.4	21
83	Storm-time plasma signatures observed by IMAGE/MENA and comparison with a global physics-based model. Geophysical Research Letters, 2005, 32, .	4.0	20
84	Simultaneous eventâ€specific estimates of transport, loss, and source rates for relativistic outer radiation belt electrons. Journal of Geophysical Research: Space Physics, 2017, 122, 3354-3373.	2.4	18
85	Relativistic electron response to the combined magnetospheric impact of a coronal mass ejection overlapping with a highâ€speed stream: Van Allen Probes observations. Journal of Geophysical Research: Space Physics, 2015, 120, 7629-7641.	2.4	17
86	The complex nature of storm-time ion dynamics: Transport and local acceleration. Geophysical Research Letters, 2016, 43, 10,059-10,067.	4.0	17
87	Ps 6 disturbances: relation to substorms and the auroral oval. Annales Geophysicae, 2003, 21, 493-508.	1.6	16
88	Association of energetic neutral atom bursts and magnetospheric substorms. Journal of Geophysical Research, 2000, 105, 18753-18763.	3.3	15
89	Transport of plasma sheet material to the inner magnetosphere. Geophysical Research Letters, 2007, 34,	4.0	15
90	Ring current pressure estimation with RAM CB using data assimilation and Van Allen Probe flux data. Geophysical Research Letters, 2016, 43, 11,948.	4.0	14

#	Article	IF	CITATIONS
91	Forecasting and remote sensing outer belt relativistic electrons from low Earth orbit. Geophysical Research Letters, 2016, 43, 1031-1038.	4.0	14
92	Observations of auroral substorms occurring together with preexisting "quiet time―auroral patterns. Journal of Geophysical Research, 1996, 101, 24621-24640.	3.3	13
93	Helium, Oxygen, Proton, and Electron (HOPE) Mass Spectrometer for the Radiation Belt Storm Probes Mission. , 2013, , 423-484.		13
94	O+ Transport into the ring current: Storm versus substorm. Geophysical Monograph Series, 2003, , 59-73.	0.1	12
95	The Evolution of the Plasma Sheet Ion Composition: Storms and Recoveries. Journal of Geophysical Research: Space Physics, 2017, 122, 12,040.	2.4	12
96	Comparison of Viking onset locations with the predictions of the Thermal Catastrophe Model. Journal of Geophysical Research, 1995, 100, 21857-21872.	3.3	11
97	Calculation of IMAGE/MENA geometric factors and conversion of images to units of integral and differential flux. Review of Scientific Instruments, 2005, 76, 043303.	1.3	11
98	Extension of an Empirical Electron Flux Model From 6 to 20 Earth Radii Using Cluster/RAPID Observations. Space Weather, 2019, 17, 778-792.	3.7	11
99	Solving the auroral-arc-generator question by using an electron beam to unambiguously connect critical magnetospheric measurements to auroral images. Journal of Atmospheric and Solar-Terrestrial Physics, 2020, 206, 105310.	1.6	11
100	Special features of a substorm during high solar wind dynamic pressure. Journal of Geophysical Research, 1995, 100, 19095.	3.3	10
101	Polar CEPPAD/IPS energetic neutral atom (ENA) images of a substorm injection. Advances in Space Research, 2000, 25, 2407-2416.	2.6	10
102	Unusually quick development of a 4000 nT substorm during the initial 10 min of the 29 October 2003 magnetic storm. Journal of Geophysical Research, 2006, 111, .	3.3	10
103	Substorm Associated Spikes in High Energy Particle Precipitation. Geophysical Monograph Series, 0, , 227-236.	0.1	10
104	A 2-D empirical plasma sheet pressure model for substorm growth phase using the Support Vector Regression Machine. Journal of Geophysical Research: Space Physics, 2015, 120, 1957-1973.	2.4	10
105	SAPSâ€Associated Explosive Brightening on the Duskside: A New Type of Onset‣ike Disturbance. Journal of Geophysical Research: Space Physics, 2018, 123, 197-210.	2.4	10
106	Key features of intense geospace storms—A comparative study of a solar maximum and a solar minimum storm. Planetary and Space Science, 2007, 55, 32-52.	1.7	9
107	Modeling the ring current response to a sawtooth oscillation event. Journal of Atmospheric and Solar-Terrestrial Physics, 2007, 69, 67-76.	1.6	9
108	Improved Simulations of The Inner Magnetosphere During High Geomagnetic Activity With the RAMâ€SCB Model. Journal of Geophysical Research: Space Physics, 2019, 124, 4233-4248.	2.4	8

#	Article	IF	CITATIONS
109	Why Are There so Few Reports of Highâ€Energy Electron Drift Resonances? Role of Radial Phase Space Density Gradients. Journal of Geophysical Research: Space Physics, 2020, 125, e2020JA027924.	2.4	8
110	A Mission Concept to Determine the Magnetospheric Causes of Aurora. Frontiers in Astronomy and Space Sciences, 2020, 7, .	2.8	8
111	Magnetotail Dipolarizations and Ion Flux Variations During the Main Phase of Magnetic Storms. Journal of Geophysical Research: Space Physics, 2021, 126, e2020JA028470.	2.4	8
112	Science Goals and Overview of the Radiation Belt Storm Probes (RBSP) Energetic Particle, Composition, and Thermal Plasma (ECT) Suite on NASA's Van Allen Probes Mission. , 2013, , 311-336.		8
113	How whistler mode hiss waves and the plasmasphere drive the quiet decay of radiation belts electrons following a geomagnetic storm. Journal of Physics: Conference Series, 2020, 1623, 012005.	0.4	8
114	Toward understanding radiation belt dynamics, nuclear explosion-produced artificial belts, and active radiation belt remediation: Producing a radiation belt data assimilation model. Geophysical Monograph Series, 2005, , 221-235.	0.1	7
115	Cluster magnetotail observations of a tailward-travelling plasmoid at substorm expansion phase onset and field aligned currents in the plasma sheet boundary layer. Annales Geophysicae, 2005, 23, 3667-3683.	1.6	7
116	Geospace Plume and Its Impact on Dayside Magnetopause Reconnection Rate. Journal of Geophysical Research: Space Physics, 2021, 126, e2021JA029117.	2.4	7
117	Prelude to THEMIS tail conjunction study. Annales Geophysicae, 2007, 25, 1001-1009.	1.6	6
118	"Snowplow―injection front effects. Journal of Geophysical Research: Space Physics, 2013, 118, 6478-6488.	2.4	6
119	Recurrent embedded substorms during the 19 October 1998 GEM storm. Journal of Geophysical Research: Space Physics, 2016, 121, 7847-7859.	2.4	6
120	Magnetospheric solitary structure maintained by 3000 km/s ions as a cause of westward moving auroral bulge at 19 MLT. Annales Geophysicae, 2009, 27, 2947-2969.	1.6	6
121	Global auroral imaging in the ILWS era. Advances in Space Research, 2007, 40, 409-418.	2.6	5
122	Effects of a Realistic O ⁺ Source on Modeling the Ring Current. Journal of Geophysical Research: Space Physics, 2019, 124, 9953-9962.	2.4	5
123	On-orbit calibration of geostationary electron and proton flux observations for augmentation of an existing empirical radiation model. Journal of Space Weather and Space Climate, 2020, 10, 28.	3.3	5
124	The Cold Ion Population at Geosynchronous Orbit and Transport to the Dayside Magnetopause: September 2015 to February 2016. Journal of Geophysical Research: Space Physics, 2019, 124, 8685-8694.	2.4	4
125	Defining Radiation Belt Enhancement Events Based on Probability Distributions. Space Weather, 2020, 18, e2020SW002528.	3.7	4
126	Generation of Subauroral Longitudinally Extended Emissions Following Intensifications of the Poleward Boundary of the Substorm Bulge and Streamer Production. Journal of Geophysical Research: Space Physics, 2021, 126, e2020JA028556.	2.4	4

#	Article	IF	CITATIONS
127	Energetic neutral atom imaging with the polar ceppad/ips instrument: Initial forward modeling results. Physics and Chemistry of the Earth, Part C: Solar, Terrestrial and Planetary Science, 1999, 24, 203-208.	0.2	3
128	Simultaneous closed magnetic field line polar arcs and substorms. Journal of Atmospheric and Solar-Terrestrial Physics, 2001, 63, 643-655.	1.6	3
129	Highly periodic stormtime activations observed by THEMIS prior to substorm onset. Geophysical Research Letters, 2008, 35, .	4.0	3
130	Comment on "Investigation of the period of sawtooth events―by X. Cai and C. R. Clauer. Journal of Geophysical Research, 2010, 115, .	3.3	3
131	Los Alamos Geosynchronous Space Weather Data for Radiation Belt Modeling. Geophysical Monograph Series, 0, , 237-240.	0.1	3
132	Particle tracing modeling of ion fluxes at geosynchronous orbit. Journal of Atmospheric and Solar-Terrestrial Physics, 2018, 177, 131-140.	1.6	3
133	Key elements of auroral substorm development and their relationship to recent observations of detached sub-auroral phenomena including STEVE-like emissions. Journal of Atmospheric and Solar-Terrestrial Physics, 2021, 218, 105600.	1.6	3
134	The Role and Contributions of Energetic Neutral Atom (ENA) Imaging in Magnetospheric Substorm Research. , 2003, , 155-182.		2
135	Determination of errors in derived magnetic field directions in geosynchronous orbit: results from a statistical approach. Annales Geophysicae, 2016, 34, 831-843.	1.6	2
136	Association of Mesoscale Auroral Structures and Breakups With Energetic Particle Injections at Geosynchronous Orbit. Frontiers in Astronomy and Space Sciences, 0, 9, .	2.8	2
137	Viking observations of a reverse convection cell developing in response to a northward turning of the interplanetary magnetic field. Geophysical Research Letters, 1996, 23, 809-812.	4.0	1
138	Observations of dipolarization at geosynchronous orbits and its response in the polar cap convection during extreme southward interplanetary magnetic field conditions. Journal of Geophysical Research, 2007, 112, .	3.3	1
139	Calculating Ionizing Doses in Geosynchronous Orbit from In-situ Particle Measurements and Models. , 2020, , .		1
140	Long-term energetic-particle databases from geosynchronous and GPS orbits. , 0, , .		0
141	Acceleration and loss driven by VLF chorus: Van Allen Probes observations and DREAM model results. , 2014, , .		0
142	Data assimilation of space-based and ground-based observations, and empirical models into a plasmasphere model. , 2014, , .		0
143	Topological Segmentation and Tracking for Space Weather Modeling. , 2021, , .		0